Multimaterial Manufacture Through Combining Optical Tweezers with Multiphoton Fabrication

M. Askari, C. J. Tuck, Q. Hu, R. J. M. Hague and R. D. Wildman

Faculty of Engineering, The University of Nottingham, University Park, NG7 2RD, UK
Email: Meisam.askari@nottingham.ac.uk

Multi-Photon Polymerization (MPP) is a technique used to fabricate complex micro-scale 3D structures using ultra-short laser pulses. Typically, MPP is used to manufacture micron-scale components in photopolymer materials. However, the development of micron scale processes that can produce components from multiple materials within a single manufacturing step would be advantageous. This would allow the inclusion of particles that are manipulated and embedded within structures with sub-micron feature sizes. To achieve this, an MPP system was combined with an optical trapping (OT) setup in order to independently manipulate microparticles in the x, y and z planes. Particles were transported into the fabrication site using the OT and encapsulated using the MPP laser. Here it is shown that combining the OT capabilities with an additive manufacturing technique enables the production of complex multi-material artifacts.

DOI: 10.2961/jlmn.2019.01.0014
Keywords: additive manufacturing, multi-photon polymerization, optical trapping, direct laser writing, hybrid structures, 3D printing, two-photon polymerization, optical tweezers.

1. Introduction

Additive Manufacturing (AM) or 3D printing is the technology of building three-dimensional objects layer-by-layer using computer-aided designs [1]. It is capable of fabricating complex three-dimensional designs, which cannot be fabricated using conventional manufacturing techniques. Recently, there has been a considerable effort in extending AM to afford multimaterial fabrication, for the provision of multiple functions within an object [2–4]. One example of a multifunctional AM (MFAM) is the production of active components. An active component includes mechanical, electrical, optical or other functional properties [5,6]. Should MFAM be realized, it will lead to a raft of new AM-based applications in a range of sectors including electronics, bioprinting/tissue engineering and the pharmaceutical industries.

Functional microscale structures can improve the response time of the sensors to an external stimulus. Therefore, it is beneficial to take MFAM from millimetre to micron scale [7]. A powerful route for manufacturing 3D structures with sub-µm resolution is Multi-Photon Polymerization (MPP) [8][9]. MPP is a 3D manufacturing technique and has higher fabrication speed and larger build area when compared to more established sub-micron 2D patterning technologies such as Electron Beam Lithography (EBL) [10].In particular, it can be used to fabricate structures without the need for expensive clean rooms, masks/tooling and can be conducted at atmospheric pressures. The working principle of MPP is based on the absorption of multiple photons in the infrared range to replace a single photon in the ultraviolet range [11] in suitable photochemical systems. The accumulated energy of multiple photons is sufficient to produce free radicals from photoinitiators that are present within a monomer/photoinitiator fluid. The free radicals react with the monomers and produce the activated monomer or the chain carrier. The activated monomer rapidly reacts with other monomers and produce a polymer chain with higher molecular weight [11–13]. The degree of monomer to polymer conversion can be controlled using the MPP processing parameters. Therefore, the material properties can also be tuned using the processing parameters [14].

MPP is a third order nonlinear effect [15] and the rate of light absorption is proportional to the square of the incident light intensity [12]. The excitation beam intensity should be in the order of ~1 TW/cm^2 to surpass the polymerization threshold for multiphoton polymerization [16]. Reaching photon density comparable with molecular density can also produce free radical generation through direct photo-cleavage of the chemical bonds that compete with other polymerization mechanisms [17].

For example, a Ti-Sapphire femtosecond laser focused by an oil immersion objective lens can produce sufficient photon density to initiate polymerization in the resin. Using a TEM_{00} beam with a Gaussian beam profile restricts the polymerization region to the centre of the focal volume of the objective lens. This increases the resolution of the setup [13,18]. To date, MPP has primarily been used as a single material system and using more than one material in a structure fabricated in MPP requires consecutive development and fabrication cycles for each material [7,19,20]. Composite structures have been achieved by sequential MPP fabrication of structures with materials that have different reactivity. Subsequent chemical activation of the fabricated structures enables site selective metallization of these structure [21–25]. Another popular technique in fabrication of composite structures using MPP is by adding fine ceramic, metallic particles and carbon nanotubes to the photoresist [26,27].

Subsequent polymerization is proven to be a challenging process due to difficulties in aligning the system with samples that has pre-existing features. Also, handling printed micron size objects is not practical. Saha et al. suggested the use of a bespoke kinematic mount that enables sample handling and alignment in different stages of fabrication [20].

To reduce the intermediate steps in fabrication of composite structures, it is possible to merge MPP with another technique that can provide in situ material tailoring.

One possible route to combining materials of a different type and crucially different length scales is utilising Optical Trapping (OT) for manipulating μm size objects. Optical tweezers use an oil immersion objective lens to produce a highly focused laser beam. The interaction of the laser beam with the particles close to its beam waist produces a net trapping force [28] which can then be used to manipulate the particle. Since its inception, OT technology has been used for manipulating many types of materials, including silica particles [29], gold nanorods [30], biological samples [29] and DNA strands [31].

The combined OT and MPP setup is a highly selective technique that can incorporate particles in the specific area of a design and tailor the properties of that area. The other advantage of the combined MPP and OT setup is in the elimination of intermediate steps. This technique can fabricate composite structure is one process. Therefore, there is no need for sequential polymerization and post-processing steps like polymer activation.

There are two seminal papers that demonstrate the simultaneous utilisation of OT and MPP. Dawood et al. showed the combination of MPP and OT and successfully spot welded 5 μm silica microbeads to a substrate using MPP [32]. They also demonstrated the ability to immobilise particles on top of each other to produce a particular design. In this paper, they achieved high particle placement accuracy and polymerization resolution. This paper paves the way for further study on the combined MPP and OT technique.

Tsai et al. demonstrated the generation of nanostructures using optical trapping assisted nanopatterning [33]. They developed a new method to use a spherical microbead, which is held in place using OT, as a microlens to enhance the resolution of the MPP system. Using near-field polymerization allowed them to achieve high resolution [33]. The simulation that was done in this work demonstrated the ability of their system to use different sized spherical beads to focus the polymerization laser. The simulation results predicted that by using a larger particle (5 μm beads instead of their the primary 3 μm particles), the polymerization occurs further from the particle surface and reduces the risk of the particle being 'glued' to the substrate [33]. In the follow-up paper published by Leitz et al., they demonstrated that by placing the trapped particle very close to the substrate, similar to the case of spot welding the particle to the substrate, polymerization area is placed inside the substrate and solidification does not occur [34].

By comparing the structures fabricated by Dawood et al. and Tsai et al. it is clear that the position of the trapped particle in relation to the polymerization area is an important factor [32,33]. Polymerization and trapping occur at the focal volume of the objective lens. The position of the focal volume of the objective lens is commonly defined by the working distance of the objective lens. The working distance of an objective lens can vary based on the beam profile and the wavelength of the beam.

The fixed beam OT systems used by Tsai et al. and Dawood et al. were not able to move the trapped particle independently and the position of the trapped particle was fixed in 3D. Tsai et al. used mechanical means to align the trapping beam with the polymerization laser beam [33]. The Galvo Mirrors (GM) used by Dawood et al. for the polymerization laser, enabled Dawood et al. to align the polymerization beam with the trapping beam in the imaging plane. In both experiments the trapped particle was in a fixed distance from the objective lens. Consequently, It was not possible adjust the the gap between the polymerization and trapping area in the laser propagation direction. Dawood et al. utilized a trapping laser with a wavelength close to the polymerization wavelength and placed the trapped particle close to the polymerization area and spot-weld the particle to the substrate [32]. In contrast, Tsai et al. managed to avoid particle adhesion by utilising a trapping laser with longer wavelength. In the case of Tsai et al., due to the chromatic aberration in the system, the trapped particle was placed further from the polymerization area and acted as a microlens [33].

In this work, it was attempted to bridge the gap between the work done by Dawood et al. and Tsai et al., and develop a more versatile technique to be used with a wide range of photoresists and particles. In contrast to previous papers, the OTsetup used in this experiment utilizes a GM system with an afocal beam expander that enabled the system to move the trapped particle independently. The working distance correction which was facilitated by an independent 3D trap enables precise alignment between the polymerization and trapping areas.

The centre part of this system was an afocal beam expander that can control the position of the particle in the laser propagation direction. The afocal beam expander compensates for the difference in the working distance of the objective lens for the trapping and polymerization lasers, which relaxes the limitations in the trapping and polymerization wavelengths. Not being limited to a particular wavelength enables the researchers to use different photoresists with different polymerization wavelengths without the need to change the trapping laser wavelength. This system also enables the researchers to choose the most suitable wavelength for their experiment to reduces the optical damage to their samples or increases the wavelength dependent trapping force for the trapped particle [35].

This paper will demonstrate trapping and polymerization of soda-lime glass beads and melamine resin fluorescent particles suspended in the prepared photoresist thereby setting the precedent for use in a variety of commercially available photoresists. It will be shown that precise embedding of microparticles into a polymer matrix was possible by encasing arrays of particles into MPP fabricated 3D structures.

2. Methodology

To be able to demonstrate the hybridization of MPP and OT, the methodology taken was first to develop two independent systems and validate their capabilities. Once these facilities were operating at an acceptable precision, the two systems were integrated, tested and their combined capabilities demonstrated.

2.1. System development

The schematic diagram of the developed setup is shown in Fig. 1. This setup consists of two separate sections, which was assembled and tested independently before integration. The OT section of the setup was designed to have the

minimum number of common elements with the MPP section. Therefore, System alignment, benchmarking and modification were simpler. In the combined setup, the single objective lens was used to focus both the polymerization and the trapping laser beam onto the sample.

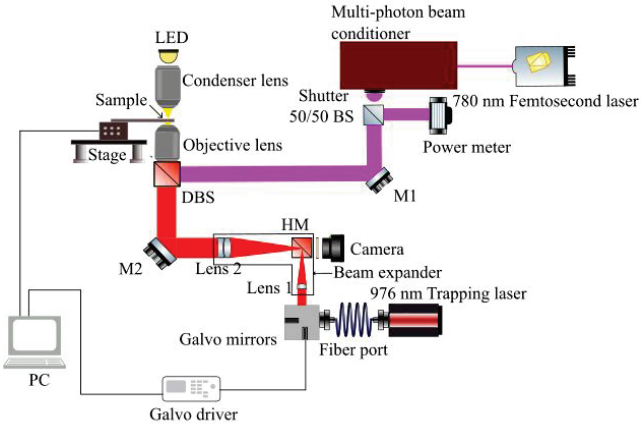

Fig. 1 Schematic illustration of the combining OT and MPP setup used during the experiment.

A Ti-Sapphire femtosecond laser (Coherent Chameleon XR) was used as the polymerizing light source. The Coherent Chameleon XR is a mode-locked broadband laser with 80 MHz repetition rate and 140 fs pulse width. The maximum output power of this laser was 4.1 W at 780 nm wavelength. The highly collimated laser output goes through a multi-photon beam conditioner (Thorlabs MPM-BCU). The beam conditioner box expands the laser beam to fill the objective lens back aperture and decreases the laser power. A Thorlabs DLMP900T Dichroic Beam Splitter (DBS) was used to reflect the polymerization laser beam towards the objective lens. The DBS has 98% transmission at 780 nm, and it was transparent to the trapping laser beam. DBS was used to combine the trapping and polymerization laser beams.

The laser beam was focused on the sample using an oil immersion objective lens (Olympus RMS100X-PFO, NA 1.30 and working distance 0.2 mm). The experimental setup was a fixed beam MPP rig and a piezoelectric stage (Physik Instrumente P-615 NanoCube XYZ Piezo System) was used to move the sample and build complex structures layer by layer. A microscope slide holder (Thorlabs MAX3SLH) was mounted to the stage using a conversion plate. Zeiss coverslips (number 1, 22 mm x 22mm) were used as a substrate. To mount the coverslip into a microscope slide holder a customised coverslip mount was designed and printed using a Stratasys Connex 260 3D printer.

The optical trapping section was based on a Thorlabs optical trapping module. This setup used a 975 nm butterfly laser diode (Thorlabs DBR976S). The Galvo Mirrors (GM) system (Thorlabs GVS102) was used to control the position of the trapping beam using the galvanometer drivers, which were connected to the analogue output of an NI DAQ device.

An afocal Keplerian beam expander was used to expand the laser beam reflected by the GM system, an. A cage translation mount (Thorlabs CT1) was used to mount the first lens in the Keplerian beam expander. This translation mount enables precise positioning of the first lens to decrease or increase the distance between the lenses in the beam expander.

2.2. Sample preparation and testing

To produce the photoresist for the combined setup 0.75 wt/vol% of commercial photoinitiator 2-Benzyl-2-(dimethylamino)-4`-morpholinobutyrophenone was added to an equal mixture of Polyethylene (Glycol) Diacrylate (PEGDA) with a molecular weight of 575 and 250. The lower molecular weight PEGDA was used to reduce the viscosity of the photoresist to 26 cP. After structure fabrication, the excess monomer was washed away using deionized water and subsequently acetone.

In this experiment, high refractive index melamine resin beads (Sigma-Aldrich FITC marked carboxylate modified) with a refractive index of 1.68 at 589 nm were manipulated into the field of view of the MPP. These particles were purchased in suspended form with 2.5% solid. 0.25 vol/vol % of the purchased solution was added to the 2 mL of the prepared photoresist and placed in an ultrasonic bath for 30 minutes. The ratio of the refractive index of the particle over its surrounding medium is 1.145, which has been reported to be sufficient to produce stable trapping [28]. Second sets of particles (Soda-lime glass beads) were also tested in this experiment (900 series Thermo Scientific). Glass beads are proven to be very desirable for enzyme immobilisation in particle-based biosensors due to their high mechanical and chemical stability [36]. The refractive index of soda-lime glass beads are 1.59 at 589.3 nm (1.08 times of the surrounding medium) which is sufficient for trapping, but their low wettability made it challenging to suspend in the photoresist. Isopropanol slurry was created before adding the particles to the photoresist to reduce agglomeration in the solution.

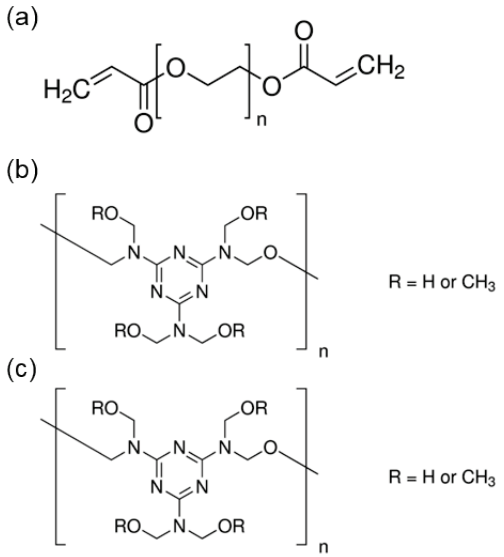

Fig. 2 Molecular structure of (a) PEGDA , (b) Melamine resin and (c) photoinitiator.

2.3 Combined setup optimization

A droplet of the prepared photoresist was placed on a coverslip, which was then fixed to the piezoelectric stage using a microscope slide holder. The first step in optimising

the combined setup was to find the interface between the resin and substrate. After locating the substrate, the polymerization beam position was recorded via the camera feed. These coordinates were used to position the optical trap using the GM.

Using the GM, the trapping laser was shifted toward a particle suspended in the polymer and the trapped particle then moved close to the polymerization area. To be able to immobilise the trapped particle within the polymer, the particle must be close to the polymerization area. In the imaging plane (X and Y), this could be achieved using a LabVIEW code that enabled a user to control the position of the trap using the mouse pointer or by manually entering the coordinates for the polymerization area. Stable optical trapping occurs in the centre of the beam waist. Therefore, the working distance of the objective lens fixes the position of the particle in the laser propagation direction [28]. Due to the chromatic aberration, the working distance of the objective lens is dependent on the laser wavelength. Fig. 3 shows an illustration of the issue where the particle trapped using the 975 nm laser is positioned above the polymerization voxel solidified using 780 nm femtosecond laser. The afocal beam expander used to expand the trapping laser beam was used to decrease the working distance of the objective lens for the trapping laser. Fig. 4 demonstrates the working principle of the afocal beam expander. The afocal beam expander enables the system to be able to polymerize photoresists that may need shorter wavelengths for polymerization (for example SU-8 with a polymerization wavelength of 520 nm [37]). It also makes it possible to use longer wavelengths for trapping particles to avoid thermal damage and bubble formation caused by a CW laser.

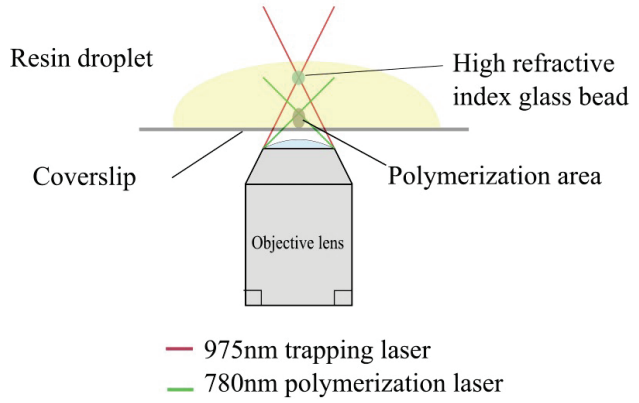

Fig. 3 Illustration of the objective lens and position of the trapped particle with respect to the polymerization area and the coverslip.

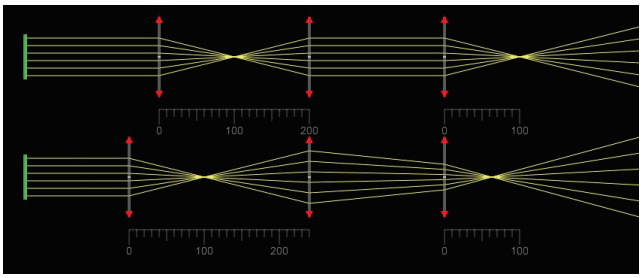

Fig. 4 Ray-optic diagram of an afocal beam expander and the effect of increasing the distance between the first and second lens in the beam expander.

To be able to adjust the working distance of the trapping laser a reference particle was trapped and pushed down to adhere to the substrate. Using the MPP laser a simple structure was fabricated on the substrate close to the reference particle to make sure that the polymerization laser beam is on the substrate and the stage Z value was recorded. Using the GM a single particle was trapped and by adjusting the first lens in the Keplerian beam expander, the particle was moved toward the substrate without moving the stage. The imaging section of the combined setup made it possible to check the position of the trapped particle by comparing the particle in the trap with the reference particle that adhered to the substrate and the structure fabricated using the MPP.

By moving the lenses and increasing/decreasing the gap between the first and second lens in the beam expander the trapping beam quality decreases. The femtosecond laser also affected the trapped particle. The trapping laser driving current was increased to 120 mA to ensure stable trapping of particles during the experiment.

Optical microscopy (Nikon, Nikon Eclipse Lv100NDP), Scanning Electron Microscopy (SEM) (Philips XL30 FEG SEM) and Time of Flight-Secondary Ion Mass Spectrometer TOF-SIMS (ION-TOF GmbH) were used to characterise the samples fabricated during this experiment.

3. Results and discussion

The accumulative energy of the trapping and the polymerization laser increases the polymer temperature near the fabrication area and bubble formations can occur. The trapping laser power was reduced to prevent bubble formation without sacrificing fabrication speed. Reducing the trapping laser power to 31.3 mW (measured before entry into the objective lens) largely reduced the bubble formation in the system. Efficient 3D trapping of melamine resin particles with 31.3 mW laser power was possible but it reduced the trapping force and particle transportation speed to 18 $\mu m/s$.

Trapping force can be calculated by considering the balance of Stokes' drag force and trapping force when a particle is manipulated [38]. To be able to accurately measure the particle movement speed the piezoelectric stage was used and instead of moving the particle using the GM, the stage moved the sample while the trapped particle was stationery. By increasing the stage speed the Stokes' drag force generated by the liquid eventually dislocated the particle from the trap. Based on the stage speed and the viscosity of the surrounding medium (the photoresist) the trapping force was calculated. Using 2.6 µm Melamine beads the maximum transportation speed was 19 $\mu m/s$. In this speed, the force acting against the trapping force dislocated the particle from the trap after a few seconds of moving in the photoresist. Therefore, the trapping force generated using the laser power of 31.3 mW was 14.7 fN.

3.1 Using the combined setup in the fabrication of 2D structures

The first experiment was designed to demonstrate the 2D capabilities of the combined setup. Attaching single particles to the substrate via MPP demonstrates that:

1) Single particles can be trapped and transported into the polymerization area.

2) The femtosecond laser solidifies the polymer around the particle in the trap.
3) The solidified polymer locks the particle in position during the development process.

During optical trapping optimisation, the trap position was overplayed on top of the polymerization area. To be able to immobilise the particles, the single particle was trapped and transported to the fabrication site using the OT. By moving the particle in the Z direction and operating the mechanical shutter the femtosecond laser solidifies the polymer between the particle and the substrate and immobilises the particle on the substrate. Having a 3D stable trap the particles could be trapped stably for an extended period of time but usually, particles are transported and immobilised in a short period. Using low density of particles in the photoresist (0.0062% solid) increased the fabrication time and it became harder to find particles to embed in the structure, but it reduces the difficulties in sample development. Particles not used in fabrication can adhere to the fabricated structures and contaminate the sample.

Fig. 5 shows the bright field microscope image of a 6 by 6 array of particles fixed to the substrate using MPP. The spherical particles are easily distinguishable, but polymer welds are too small to be resolved. Higher resolution imaging using SEM was needed to be able to observe the polymer. Fig. 6 shows an SEM picture of an array of particles fixed to the substrate using MPP. In this picture, the sample is tilted by 15 degrees to show the polymer voxels that attach the particles to the substrate.

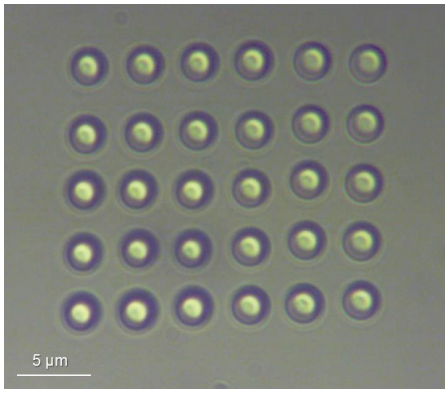

Fig. 5 Array of melamine resin microbeads placed 5 µm apart and attached to the coverslip using multiphoton polymerization of PEGDA, fabricated with a laser power of 14.55 mW and exposure time of 300 ms.

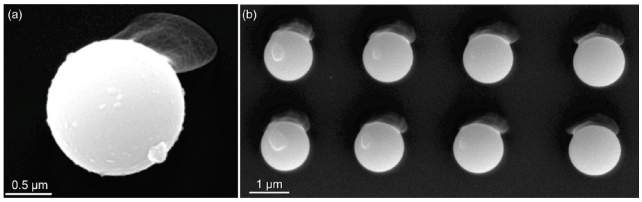

Fig. 6 SEM image (15° tilt) of an array of particles fixed to the substrate using MPP laser power 14.55 mW and exposure time of 300ms.(a) Soda-lime particle and (b) Melamine microbead.

Fig. 6a shows high refractive index soda-lime microparticles immobilised on the substrate using the MPP laser. Soda-lime particles had a lower refractive index compared to the melamine microbeads. The difference between the refractive index of the photoresist and the particle affects the trapping force. It was experimentally observed that the using similar laser trapping power soda-lime particles were less stable in the trap comparing to the melamine resin particles. Therefore, the trapping laser driving current increased to 150 mA (42.2 mW) to compensate for the lower refractive index of soda-lime particles. Higher laser power used in this experiment enabled the system to transport particles with the similar speed of 20 µm/s and produce trapping force of 9.8 fN for smaller particles with lower refractive index. It is possible to use the combined setup to manipulate a variety of particles suspended in the photoresist, as long as the refractive index of the particles is higher than the refractive index of the photoresist.

3.2 Fabrication of 3D structures

The second experiment was designed to use the full capabilities of the combined setup by embedding particles in different layers of a 3D structure and producing different patterns using particles. In this experiment using the MPP mode, fishnet structures with 5 µm openings were fabricated. The OT was used to transported particles over the fabricated structure and placed in the openings. After positioning the particle, MPP laser was used to attach the particle to the substrate. Fig. 7(a) shows the bright field image of an array of particles placed inside a fishnet structure and fixed to the substrate. To complete the first layer of the 3D structure, the particles must be encapsulated in the polymer. The PI stage driver software was used to raster scan the built area with 300 nm step size and travel speed of 20 µm/s. The main limiting factor for the fabrication speed is the trapping force generated by the OT and it is possible to increase the stage speed once the trapping phase is complete. By laying down multiple layers of the polymer, the fluorescent beads can be completely encapsulated in the polymer matrix. To be able to differentiate the particle inside the polymer matrix a portion of the particles is left exposed. To clearly differentiate the particles and demonstrate the ability of the OT setup in production different designs, the second set of particles is placed in between the particles in the first layer. Fig. 7(b) shows the second layer of the structure with 12 particles on the second layer. Particles in the second layer are brighter in the picture.

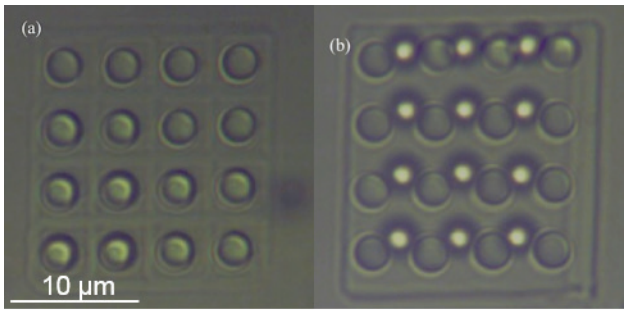

Fig. 7 Bright field microscope image of particles transported and immobilised using the combined setup. (a) The first layer of the structure with 16 particles fixed inside a fishnet structure with the MPP laser power of 14.55 mW and exposure time of 300 µs (b) Double layered structure with the second set of 12 particles locked into the fabricated structure using similar laser power.

To monitor the position of melamine fluorescent beads in the structure a confocal fluorescent microscope was used. The confocal microscope with motorised stage excited the

beads using 488 nm argon laser and imaged the structure while moving the stage in the Z direction.

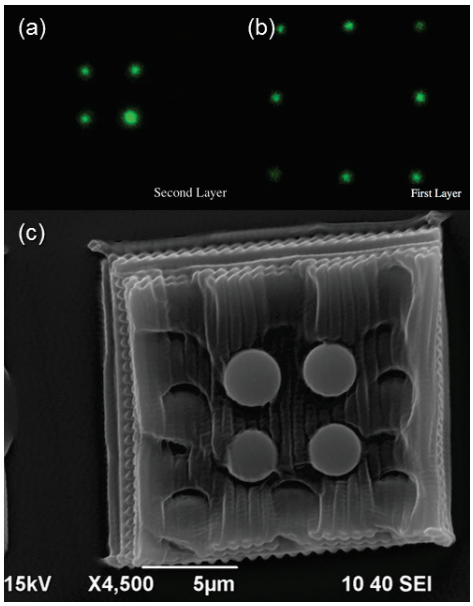

Fig. 8 Fluorescent microscope and SEM images of different layers of the structures. The green spots represent fluorescent particles in the structure. Images were taken using 63X oil immersion Nikon objective lens.

Fig.8 shows pictures taken from a structure using SEM and Fluorescent confocal microscope. Fig. 8a shows the top layer and bottom layer of the structure. The picture is taken by placing the positioning the imaging plane of the fluorescent confocal microscope in different heights from the substrate and imaging the structure in different layers. The SEM image shows the structure as a whole and the particles inside the polymer matrix is not visible.

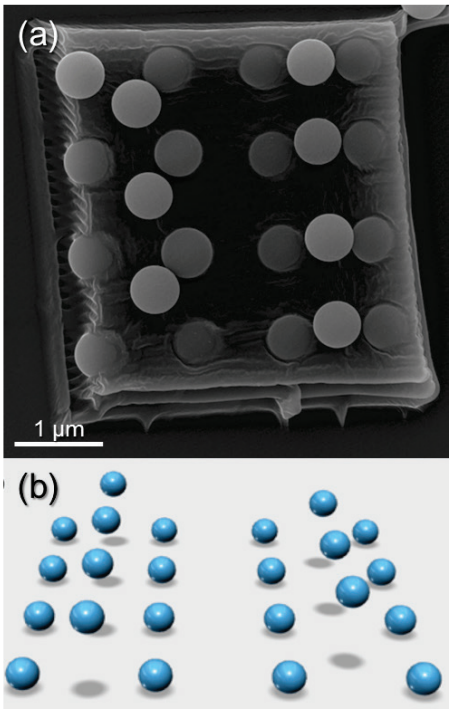

Fig. 9 SEM image of the multilayered structure with different particle arrangement particles are immobilised using MPP laser power of 14.55 mW and exposure time of 300 ms. The polymer structures are fabricated with similar laser power and stage travel speed of 20 µm. (a) Top view of the structure with 15-degree tilt, (b) CAD design showing the intended position of particles inside the structure.

Fig. 9(a) shows an SEM image of a multilayered structure fabricated. The first layer of particles is placed inside the polymer. The second set of particles is placed 2.4 µm above the first set. Fig. 9(b) is a CAD design that demonstrates the intended position of the particles that mimics' face centre cubic and body centre cubic structures.

3.3 System accuracy and repeatability

The accuracy of the combined OT and MPP system can be measured using high-resolution SEM pictures. The particles in Fig. 6 were intended to position 5 µm apart. After developing the samples and imaging, ImageJ software was used to identify particle boarders and measure the centre-to-centre distance of particles. The distance between the particles in Fig.6 was 5.6±0.5 µm in the X direction and 5.2 ± 0.1 µm in the Y direction.

Different factors contributed to the inaccuracies in the system. Positioning error, vibration and particle relocation due to polymer solidification are among the most important sources of error. Particle positioning was done using the piezoelectric stage. The drift in the stage moved the position of the immobilized particles. Therefore, consecutive particles were placed further than the intended distance. To solve this issue the piezoelectric stage was used in a closed loop system and the microscope slide was immobilized firmly using a Thorlabs microscope slide holder (MAX3SLH). In the developed system, the exposure time is controlled using a mechanical shutter and the shutter blade movement produced vibration in the system. To reduce the effect of shutter vibration, the shutter head The MPP setup minimum feature size also affects the accuracy of the system. The MPP voxel that connects the particle to the substrate moves the particles as it grows. By decreasing the MPP voxel size and disconnecting the shutter head from the 30 mm cage assembly system and mounting the mechanical shutter on a standalone table mount the effect of MPP system on the final position of the particle was minimised. Fig.10 demonstrates an array of particles immobilised on the substrate using reduced laser power. Decreasing the laser power to 11.65 mW and the exposure time to 200 ms, reducing the amount of polymer used to glue the particle to the substrate. By comparing the SEM image in Fig.6 and Fig 10, it is clear that by decreasing the minimum feature size achievable using the MPP setup, less polymer is being used to immobilize the particles and the chance of them being pushed away by the growing voxel decreases. Using ImageJ software, the distances between particles in Fig. 10 was measured. The distance between the particles in each row was 4.8±0.1 µm, which is very close to the intended 5-µm gap. The distances between neighbouring particles that are in different columns were 5.75±0.05 µm. By comparing Fig.10 and Fig 6, it is clear that measures deployed in increasing the resolution of the MPP section increased the particle placement accuracy.

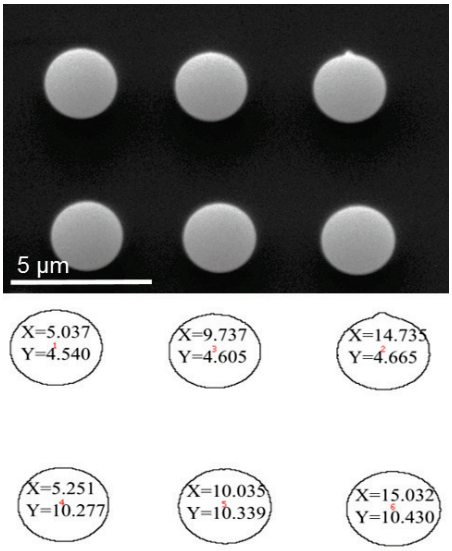

Fig.10 An array of melamine particles immobilised on the substrate using MPP laser (laser power of 11.65 and exposure time of 200ms). Particle distance in X is 4.8±0.1 µm and in Y is 5.75±0.05 µm

The inverted microscope setup used in this experiment provided a stable platform for the combined setup. The main shortcoming of this arrangement was the fact that the trapping and polymerization beam travels through the fabricated structure. The interference from the fabricated structure reduces the trapping capability of the system and limited the thickness of the structure. The thickest structures were composed of 3 layers of particles which were considered the limit for the trapping system. We didn't observe any limitation in the particle packing density in X and Y directions.

3.4 System enhancements

After the fabrication of multiple 3D structures, it was understood that the fabrication speed of the combined setup was one of the main limiting factors of the setup. Using a single-beam optical trapping and polymerization, the fabrication process explained in section 3.1 should be repeated for every single particle. To increase the fabrication speed a Holoeye DE-R 269 Diffractive Optical Element (DOE) was used to produce 7 traps in a hexagon pattern. Fig. 11 shows the optical train with DOE that enables simultaneous trapping of 7 particles.

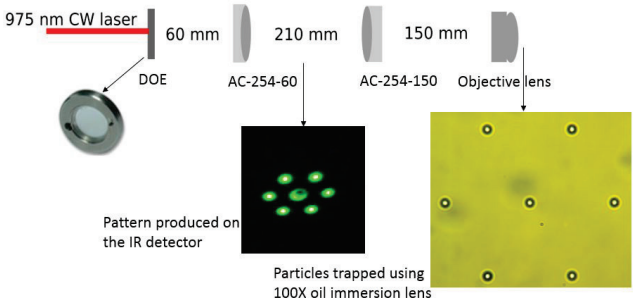

Fig. 11 DOE with a hexagonal pattern was used to split the laser beam and produce 7 trapping positions using a single laser beam. 7 particles trapped using the multiple beam optical trapping system.

Increasing the number of traps can cut the particle trapping and transportation time.

To increase the fabrication speed it is possible to use a high-speed 2D GM system instead of the piezoelectric stage to produce the patterns. Using high-speed GM, it is possible to raster scan the layers with high speed and encapsulate the trapped particles or produce specific geometries like hexagons to incorporate the particles in one scan.

To be able to stack more particles in the laser propagation direction, the combined system photoresist can be sandwiched between two coverslips. The coverslip closer to the objective lens act as a barrier between the immersion oil and the photoresist. The second coverslip will be the substrate used for sample fabrication (Fig. 12).

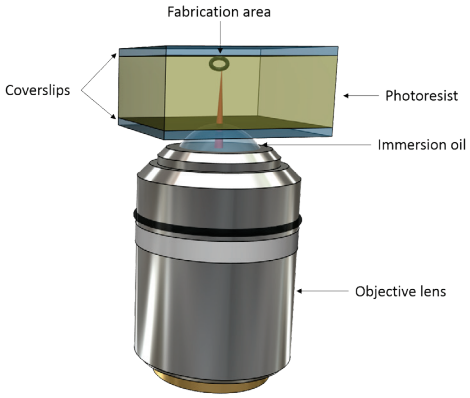

Fig. 12 schematic diagram of a proposed configuration for fabrication of composite structures. In this configuration, the fabrication and trapping laser beams are not affected by the structure.

4. Conclusion

In this paper, an OT assisted MPP setup has been demonstrated where it has been shown that it is possible to transport and embed microscopic particles into a polymer matrix fabricated using MPP. The results suggest the system enables multimaterial fabrication and gives rise to the possibility of surface modification of prefabricated structures. Using this approach, multimaterial structures can be achieved by the drawing in of objects of a variety of materials prior to polymerization and formation of a matrix, ultimately leading to a precision composite. Application areas for this approach may include fabrication of microelectromechanical systems (MEMS), biosensors and photonic bandgap structures. It was also demonstrated that a larger scale of fabrication could be achieved with multiple optical tweezers. Therefore, this setup can greatly benefit from holographic OT to transport a large number of particles in a predefined pattern to the polymerization area. It is also possible to replace the trapping laser and objective lens to trap and transport metallic particles and embed metallic particles in polymer structures.

Acknowledgements

This work was funded by the University of Nottingham and the Engineering and Physical Sciences Research Council on grant EP/I033335/2, the EPSRC Centre for Innovative Manufacturing in Additive Manufacturing. I would also like to acknowledge the help and support of Dr. David Scurr, Mr. Tim Self and Mrs. Seema Rajani.

References

[1] S.L.N. Ford: J. Int. Commer. Econ, 6 (2014) .

[2] A. Panesar, D. Brackett, I. Ashcroft, R. Wildman, R. Hague: J. Mech Des., 137 (2015).

[3] A. Stalmashonak, G. Seifert, A. Abdolvand: Ultra-Short Pulsed Laser Eng. Met. Nanocomposites, 2nd ed., Springer International Publishing, Heidelberg, 2013, pp. 5.

[4] A.F. Abouraddy, M. Bayindir, G. Benoit, S.D. Hart, K. Kuriki, N. Orf, O. Shapira, F. Sorin, B. Temelkuran, Y. Fink: Nat. Mater., 6 (2007) 336.

[5] S.B. Fuller, E.J. Wilhelm, J.M. Jacobson: J. Microelectromechanical Syst., 11 (2002) 54.

[6] J. Risner: Investigation of Dielectric Elastomer Actuation for Printable Mechatronics, University of California, Berkeley, 2008.

[7] S. Rekštyte, D. Paipulas, M. Malinauskas, V. Mizeikis: Nanotechnology, 28 (2017).

[8] C.N. LaFratta, J.T. Fourkas, T. Baldacchini, R.A. Farrer: Angew. Chemie - Int. Ed., 46 (2007) 6238.

[9] K.S. Lee, D.Y. Yang, S.H. Park, R.H. Kim: Polym. Adv. Technol., 17 (2006) 72.

[10] A. Seidel, C. Ohrt, S. Passinger, C. Reinhardt, R. Kiyan, B.N. Chichkov: J. Opt. Soc. Am. B, 26 (2009) 810.

[11] K.D. Belfield, K.J. Schafer, Y. Liu, J. Liu, X. Ren, E. Van Stryland: J. Phys. Org. Chem., 13 (2000) 837.

[12] B.H. Cumpston, S.P. Ananthavel, S. Barlow, D.L. Dyer, J.E. Ehrlich, L.L. Erskine, A.A. Heikal, S.M. Kuebler, I.Y.S. Lee, D. McCord-Maughon, J. Qin, H. Röckel, M. Rumi, X.L. Wu, S.R. Marder, J.W. Perry: Nature, 398 (1999) 51.

[13] P. Galajda, P. Ormos: Appl. Phys. Lett., 78 (2001) 249.

[14] A. Žukauskas, I. Matulaitiene, D. Paipulas, G. Niaura, M. Malinauskas, R. Gadonas: Laser Photonics Rev., 9 (2015) 706.

[15] K.D. Belfield, X. Ren, E.W. Van Stryland, D.J. Hagan, V. Dubikovsky, E.J. Miesak: J. Am. Chem. Soc., 122 (2000) 1217.

[16] S. Wu, J. Serbin, M. Gu: J. Photochem Photobiol. A Chem., 181 (2006) 1.

[17] M. Malinauskas, M. Farsari, A. Piskarskas, S. Juodkazis: Phys. Rep., 533 (2013) 1.

[18] B. Mills, D. Kundys, M. Farsari, S. Mailis, R.W. Eason: Appl. Phys. A Mater. Sci. Process., 108 (2012) 651.

[19] S. Rekštyte, E. Kaziulionyte, E. Balčiunas, D. Kaškelyte, M. Malinauskas: J. Laser Micro/Nanoeng., 9 (2014) 25.

[20] S.K. Saha, T.M. Uphaus, J.A. Cuadra, C. Divin, I.S. Ladner, K.G. Enstrom, R.M. Panas: Precis. Eng., 54 (2018) 131.

[21] N. Takeyasu, T. Tanaka, S. Kawata: Appl. Phys. A Mater. Sci. Process., 90 (2008) 205.

[22] R.A. Farrer, C.N. LaFratta, L. Li, J. Praino, M.J. Naughton, B.E.A. Saleh, M.C. Teich, J.T. Fourkas: J. Am. Chem. Soc., 128 (2006) 1796.

[23] M.M. Hossain, M. Gu: Laser Photon. Rev., 8 (2014) 233.

[24] K. Terzaki, N. Vasilantonakis, A. Gaidukeviciute, C. Reinhardt, C. Fotakis, M. Vamvakaki, M. Farsari: Opt. Mater. Express, 1 (2011) 586.

[25] T. Zandrini, S. Taniguchi, S. Maruo: Micromachines, 8 (2017).

[26] S. Ushiba, S. Shoji, K. Masui, P. Kuray, J. Kono, S. Kawata: Carbon N. Y., 59 (2013) 283.

[27] L. Li, M. Hong, M. Schmidt, M. Zhong, A. Malshe, B. Huis In'Tveld, V. Kovalenko: CIRP Ann. - Manuf. Technol., 60 (2011) 735.

[28] K.C.C. Neuman, S.M.M. Block: Rev Sci. Instrum., 75 (2004) 2787.

[29] P. Jordan, J. Cooper, G. McNay, F.T. Docherty, W.E. Smith, G. Sinclair, M.J. Padgett: Opt. Lett., 29 (2004) 2488.

[30] M. Pelton, M. Liu, H.Y. Kim, G. Smith, P. Guyot-Sionnest, N.F. Scherer: Opt. Lett., 31 (2006) 2075.

[31] V. Bormuth, A. Jannasch, M. Ander, C.M. van Kats, A. van Blaaderen, J. Howard, E. Schäffer: Opt. Express, 16 (2008) 13831.

[32] F. Dawood, S. Qin, L. Li, E.Y. Lin, J.T. Fourkas: Chem. Sci., 3 (2012) 2449.

[33] Y.C. Tsai, K.H. Leitz, R. Fardel, M. Schmidt, C.B. Arnold: Phys. Procedia, 39 (2012) 669.

[34] K.H. Leitz, Y.C. Tsai, F. Flad, E. Schäffer, U. Quentin, I. Alexeev, R. Fardel, C.B. Arnold, M. Schmidt: Appl. Phys. Lett., 102 (2013) 243108.

[35] B. Hester, G.K. Campbell, C. Lpez-Mariscal, C.L. Filgueira, R. Huschka, N.J. Halas, K. Helmerson: Rev. Sci. Instrum., 83 (2012) 043114.

[36] J.A. Thompson: Microbead-Based Biosensing in Microfluidic Devices, University of Pennsylvania, 2011.

[37] D.J. Shir, E.C. Nelson, D. Chanda, A. Brzezinski, P. V. Braun, J.A. Rogers, P. Wiltzius: J. Vac. Sci. Technol. B, Nanotechnol. Microelectron. Mater. Process. Meas. Phenom., 28 (2010) 783.

[38] L.P. Ghislain, N.A. Switz, W.W. Webb: Rev. Sci. Instrum., 65 (1994) 2762.

(Received: June 26, 2018, Accepted: February 23, 2019)